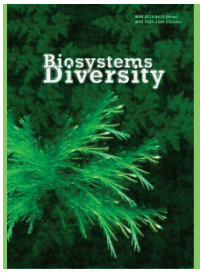

Biosystems Diversity

ISSN 2519-8513 (Print)
ISSN 2520-2529 (Online)
Biosyst. Divers.,
2023, 31(4), 428–435
doi: 10.15421/012351

Landsat archive for detection of change in Mediterranean ecosystems: The case of Northern Morocco

Y. Bouziani*, S. Lahssini**, S. Moukrim***, A. Azedou*, H. Mharzi-Alaoui****, A. Benabou***, L. Zidane*

*Ibn Tofail University, Kenitra, Morocco
**National School of Forest Engineers, Salé, Morocco
***Mohammed V University, Rabat, Morocco
****National Agency for Water and Forests, Rabat, Morocco

Article info

Received 25.08.2023
Received in revised form 02.10.2023
Accepted 14.10.2023

Ibn Tofail University, BP 133, Kenitra, Morocco. Tel.: +212-537-329-400. E-mail: adrestout@gmail.com

National School of Forest Engineers, BP 511, Salé, Morocco. Tel.: +212-537-861-149. E-mail: marghadi@gmail.com

Mohammed V University, BP 1014, Rabat, Morocco. Tel. : +212-537-778-012. E-mail: said.moukrim@fsr.um5.ac.ma

National Agency for Water and Forests, BP 20081, Rabat, Morocco. Tel.: +212-537-689-332. E-mail: hicham.mharzialaoui@gmail.com

Bouziani, Y., Lahssini, S., Moukrim, S., Azedou, A., Mharzi-Alaoui, H., Benabou, A., & Zidane, L. (2023). Landsat archive for detection of change in Mediterranean ecosystems: The case of Northern Morocco. Biosystems Diversity, 31(4), 428–435. doi:10.15421/012351

The study of changes in land cover provides a better understanding of the interactions between humans and natural ecosystems. In this context, the present study focused on the dynamics of natural ecosystems in the Rif region of Northern Morocco. The methodology was based on the inspection and visual interpretation of Landsat and Google Earth image captures, the time series of five Landsat 4-8 image bands, and the Tasseled Cap indices for a random sample of 500 points from 1984 to 2022. The study found that changes affected practically the whole study region over the study period, with around a third of them being ignored due to their very tiny magnitudes or being false positives. The findings demonstrated a general declining trend in the measured changes, indicating a reduction in pressure on different ecosystems. Furthermore, this tendency may be due in part to the availability of Google Earth images during the 2000s, which has significantly reduced the number of false positives. In terms of the year of first change, only 5.7% of pixels experienced their first events after the year 2000, implying that these pixels underwent no change for at least the first 16 years of the study period. On the other hand, 2.5% of the pixels had their last events during the first ten years and have thus remained unmodified for at least 27 years. For the year 2020, the confidence rating of the visual land cover categorization is medium to high for 88.9% of pixels using high-resolution Google Earth photos, whereas the classification quality was inadequate for 64% of pixels in 1984. Despite the stresses on the ecosystems structured by shrubs/shrubs, forests, and herbaceous/shrubs caused by the different disturbances identified, the majority of these ecosystems have not been converted to new land cover classes. According to the study, agriculture is the primary driving force underlying the conversion of forests, herbaceous/shrublands, and even shrublands/shrublands. The area increases for the latter three ecosystems represent, on the one hand, their ability to regenerate themselves and, on the other, Morocco's restoration efforts.

Keywords: biodiversity monitoring; ecosystem structure; remote sensing; land cover; time series; Google Earth Engine.

Introduction

Biodiversity encompasses the complex diversity of life at all levels from genes to ecosystems through species and the structure, function, distribution, traits, and composition of all living beings (Skidmore et al., 2021). Habitat, ecosystem, and biodiversity degradation challenge the international community to increase actions to address this problem (Sustainable Development Goals, Aichi Targets, risk assessments by the IPBES platform) (Díaz et al., 2019; Skidmore et al., 2021). Optimized biodiversity monitoring initiatives have been implemented (Scholes et al., 2012) and essential biodiversity variables (EBVs) have been defined (Pereira et al., 2013). Ecosystem structure is one of the EBV classes that include land cover, which is related to ecosystem extension and fragmentation as well as habitat disturbance belonging to the Ecosystem function class (Pereira et al., 2013; Secades et al., 2014). Land cover and its dynamics are also considered among the determinants of global CO_2 emissions (Arevalo et al., 2020); indeed, more than half of anthropogenic CO_2 emissions are attributed to land use and land cover changes (Houghton & Nassikas, 2017).

Ecosystem sustainability, climate change mitigation efforts require the study and monitoring of land use and land cover change (Gutman et al., 2004; Carpenter et al., 2006; Wulder et al., 2008). The production of global time series of land cover change has been identified by the Millennium Ecosystem Assessment as a requirement to support decision makers with information on ecosystem change. These studies also provide a better understanding of human-nature interactions and the consequences of land cover change on natural ecosystems (Turner et al., 2007) and improve knowledge of the types, magnitudes, causes, and consequences of land change (Brown et al., 2020).

The development of space technologies, tools, sensors, algorithms, and computational capabilities have been very beneficial for studies of land cover and land cover change (Brown et al., 2020; Azedou et al., 2023). Several applications of remote sensing have been developed (Arevalo et al., 2020): detection of disturbances affecting forest ecosystems (Hansen et al., 2013), assessment of regeneration dynamics and resilience (Kennedy et al., 2012), deforestation (Hamunyela et al., 2016), wetland loss (Halabisky et al., 2016), agricultural expansion (Kibret et al., 2016), urbanization (Fu & Weng, 2016), change detection (Banskota et al., 2014), etc.

Depending on the spatial and temporal scales, various data sources have been mobilized in the literature. Due to their high temporal frequency, MODIS image time series have been exploited for monitoring large-scale changes (e.g. Verbesselt et al., 2010), however, the low spatial resolution of these images reduces the ability to detect small changes (Jin & Sader, 2005), which are dominant in changes of anthropogenic origin (Zhu & Woodcock, 2014b). Landsat images have been widely used for change detection (Fu & Weng, 2016; Halabisky et al., 2016); the importance of these Landsat images resides in the free access to the archive of images produced since 1972, their spatial resolution, radiometric and geometric calibration accuracy (Wulder et al., 2012; Zhu & Woodcock, 2014a).

The detection of changes and disturbances can be based on several approaches, depending on the frequency of the images used. It can be based on the comparison of images taken at two different dates (Singh, 1989) or on the exploitation of time series judged to give better results (Coppin et al., 2004). The time series of images are exploited either by creating a composite image per year without clouds, or by merging the images ex. Landsat with MODIS to result in a clear image every 16 days, or by using metrics of multi-temporal values recorded at each pixel level such as slope or percentiles, or directly especially with dense time series allowing faster and more accurate detection (Zhu, 2017). Image exploitation can be based both on the information recorded at the level of each information band (e.g. Green, Red, NIR, SWIR1 and SWIR2: (Zhu et al., 2020)), as it can aggregate them to derive synthetic values. In this sense, various indices have been used e.g.: "Normalized Difference Vegetation Index" (NDVI) (Reed et al., 1994), "Normalized Difference Wetness Index" (NDWI) (Gao, 1996), "Tasseled Cap Wetness" (TCW) (Frazier et al., 2015), "Normalized Burn Ratio" (NBR) (Chance et al., 2016).

Morocco is known for its remarkable floristic and ecological diversity in the Mediterranean region (Benabid, 2000). Unfortunately, this biodiversity and particularly that of Rif forest ecosystems, has been exposed since the 1970s to serious disturbances if not threats of deforestation due to factors such as demographic growth, agricultural expansion, rangeland development and tourism (Benabid, 2000; Chebli et al., 2018). On the other hand, Morocco has made significant efforts to address these issues (Moukrim et al., 2019). In this context, this article provides a systematic inventory of all changes that have affected a random sample of 500 pixels representative of four Rif provinces between 1984 and 2022. The study also focuses on identifying the land cover in 1984 and 2022. Furthermore, the article investigates the dynamics of natural ecosystems as well as the exchanges with other classes of land cover in order to characterize their conditions of degradation, conservation and rehabilitation as well as the driving forces leading these dynamics. The ultimate goal is to improve the management of these ecosystems and thus increase their resilience regarding the climate change (Benabou et al., 2022; Moukrim et al., 2022). To carry out these analyses, the approach adopted is based on a meticulous visual examination and interpretation of time series, for the sampled pixels, related to Tasseled Cap indices and to 5 bands of Landsat 4-8 images covering the period 1984–2022. The examination is based on the exploitation of Landsat image extracts and high-resolution Google Earth (GE) images. These investigations are made possible by taking advantage of the powerful cloud computing platform Google Earth Engine (GEE).

Materials and methods

Study area. The study area has a total size of 9,643 km^2 and is located in the region of Tangier, Tetouan Al Hoceima in northwest Morocco, and includes the provinces of Al Hoceima, Chefchaouen, Tetouan, and M'diq-Fnideq (Fig. 1).

Structurally, the area belongs to the Rifan domain composed of Paleozoic, Secondary and Tertiary thrust sheets (Benabid, 2000). The climate is Mediterranean with the presence of almost all types of bioclimates from semi-arid to per-humid with hot, temperate, cool, cold and very cold variants (Benabid, 2000). The vegetation levels present range from the Thermomediterranean to the Mediterranean Montagnard, through the Mesomediterranean and the Supramediterranean (Benabid, 2000). The study area is part of two ecoregions, the humid forests and the sclerophyllous forests. The humid forests are organized by *Abies maroccana*, *Cedrus atlantica*, *Quercus faginea*, *Q. pyrenaica*, *Pinus clusiana* var. *mauritanica* among others (Benabid, 2000). The sclerophyllous forests are represented by the ecosystems of *Quercus rotundifolia*, *Q. suber*, *Q. coccifera*, *Olea oleaster*, *Ceratonia siliqua*, *Tetraclinis articulata*, *Juniperus phoenicea*, *Pinus halepensis*, *Pinus pinaster* var. *iberica* and *P. pinaster* var. *maghribiana* (Benabid, 2000). Also, specialized ecosystems are represented, particularly dune ecosystems organized by *Juniperus turbinata* and *Ammophila arenaria* (Benabid, 2000) and wetland ecosystems consisting of freshwater herbaceous vegetation, riparian forests or halophytes (Benabid, 2000). Also, agrosystems with a biodiversity of fauna and flora, where traditional and modern production systems coexist, are represented in the area (Benabid, 2000). This area is part of the Intercontinental Mediterranean Biosphere Reserve and includes a network of protected areas consisting of several terrestrial SIBEs and wetlands including two national parks.

Methodology. The approach adopted for the analysis of the dynamics of natural ecosystems is shown in Figure 2. It combines satellite imagery with visual interpretation of available images covering the period 1984–2021. The data employed includes the whole collection of Landsat 4-8 (4, 5, 7 and 8) satellite images, pre-processed, in the region. To understand the dynamics, a sample of 500 points was randomly selected. Time series graphs of reflectances of all bands, as well as graphs of computed Tasseled Cap indices, were created for each point, analyzed, and visually compared to the temporal dynamics of the ecosystem using available Landsat and Google Earth (GE) images. Thus, any changes identified, their intensity, and any possible conversion of land cover with respect to 1984 were analyzed and reported.

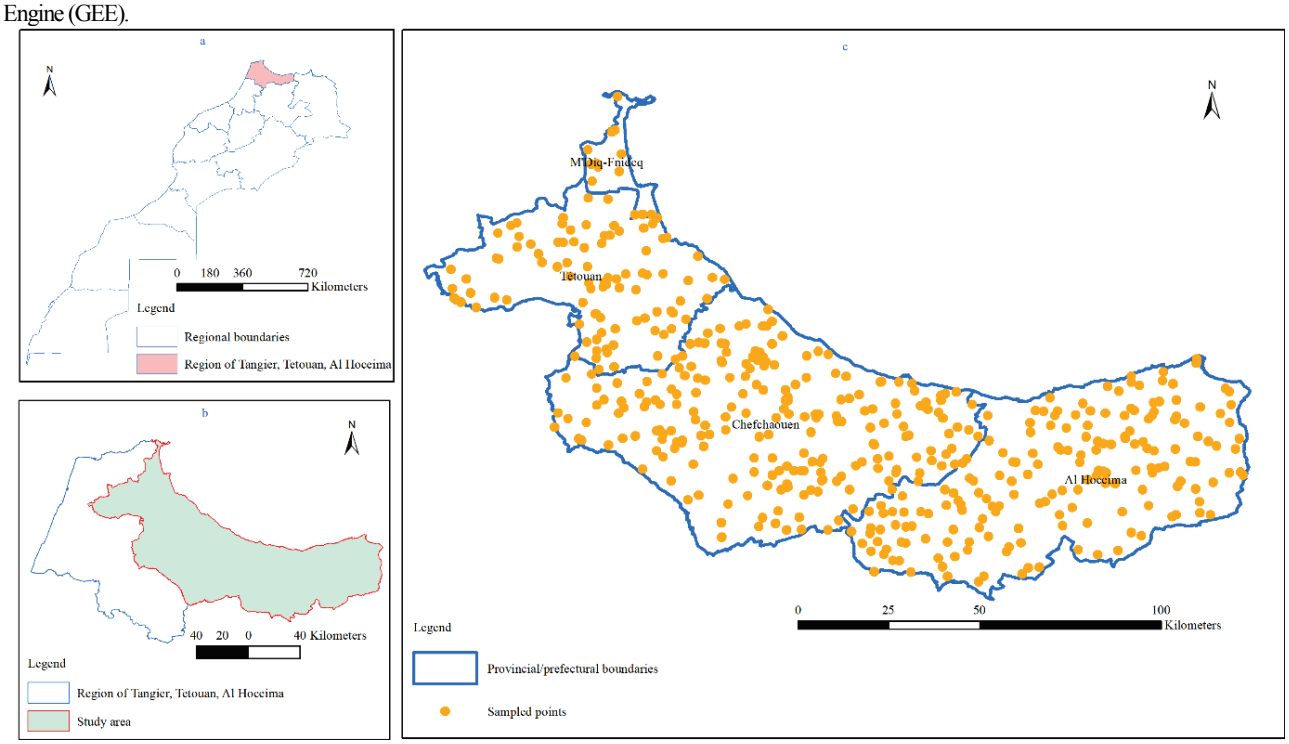

Fig. 1. Location of the study area: *a* – regions of Morocco; *b* – study area boundaries; *c* – study area with sampled points

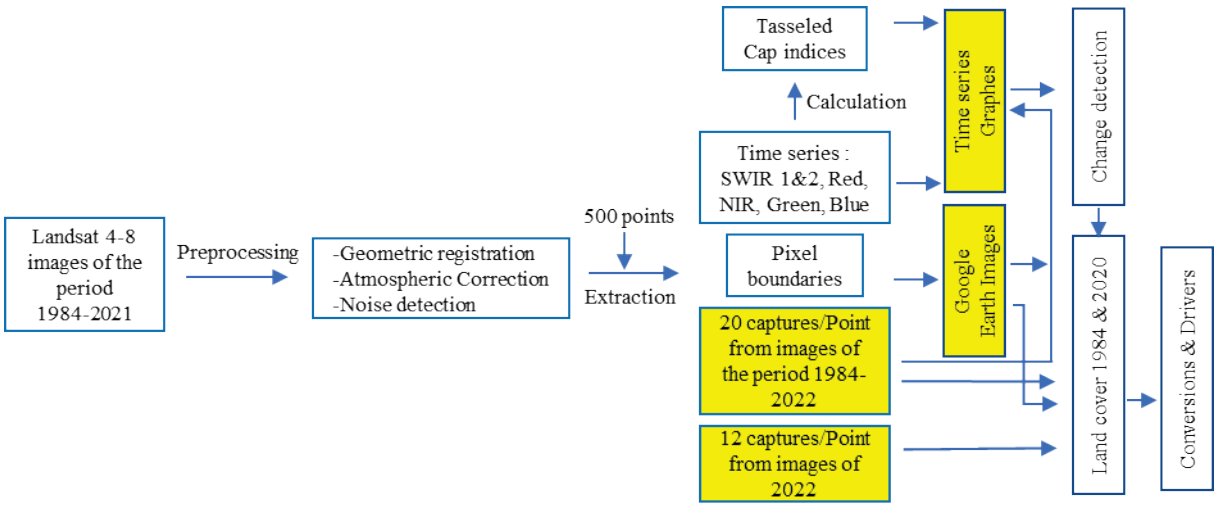

Fig. 2. Overall diagram of the methodology adopted: the yellow rectangles correspond to interpreted elements

Mobilized data. The entire collection of available L1T Landsat L4-8 images covering the study area from January 1, 1984 to December 31, 2021 was mobilized. The L1T Landsat L4-8 images were selected especially because they are available and have the highest geometric accuracy. Also, the mobilized collection has already been previously atmospherically corrected using the "Landsat Ecosystem Disturbance Adaptive Processing System" (LEDAPS) (Masek et al., 2006) and the L8SR algorithm (Vermote et al., 2016) and this respectively for the L4-7 and L8 images.

Preparation of the data sets. The detection of clouds and their shadows is essential for the detection of changes (Zhu, 2017). The use of automated cloud detection algorithms has significantly reduced the time spent on image preparation (Zhu et al., 2015), especially for the exploitation of time series (Zhu & Woodcock, 2014b). The CFMask algorithm has been used since 2016 to produce the QA (Quality Assessment) band, of the Landsat image collection 1 products (Zhu & Woodcock, 2014a; Zhu, 2017). Thus, a mask was used to remove pixels containing clouds or cloud shadows by applying the QA band.

The brightness, Greenness, and Wetness indices (Crist, 1985) were calculated and stacked as follows:

Brightness = (BLUE * 0.2043) + (GREEN * 0.4158) + (RED * 0.5524) + (NIR * 0.5741) + (SWIR1 * 0.3124) + (SWIR2 * 0.2303)

Greenness = (BLUE * (-0.1603)) + (GREEN * (-0.2819)) + (RED * (-0.4934)) + (NIR * 0.7940) + (SWIR1 * (-0.0002)) + (SWIR2 * (-0.1446))

Wetness = (BLUE * 0.0315) + (GREEN * 0.2021) + (RED * 0.3102) + (NIR * 0.1594) + (SWIR1 * (-0.6806)) + (SWIR2 * (-0.6109))

The sampled points were overlapping on the selected images to obtain the value at each date and band (SWIR1, SWIR2, Red, NIR, Green, and Blue, as well as the calculated indices of Brightness, Greenness, and Wetness). The time series for each point was compiled and graphs illustrating the historical progression of each index were generated.

Interpretation of the time series. Each point-pixel was visually assessed in order to identify potential changes during the time period covered and to identify possible land cover conversions.

Landsat image captures obtained around or on June 1st, covering even years of the study period, as well as 2021, were meticulously analyzed. In addition to visual interpretation, graphs of the progression of the various indices allow for recognition of the trend of gradual changes (e.g., greening or browning of vegetation).

High resolution GE images were used, depending on their availability, to confirm or reject the occurrence of disturbances. To validate suspicious changes identified on Landsat images or find changes that could not be observed on them, all GE images for each of the pixel-points considered were entirely consulted. The point-pixels which had the majority or totality of poor-quality images due to the presence of clouds or defects associated with the SLC (Scan Line Corrector) were removed from the time series interpretation. Thus, 59 pixel-points were excluded from the time series interpretation. For each pixel, the year as well as the nature of each change was noted. For nature of change, two types of changes can affect the land's surface: a) abrupt occurring in a short period of time with large amplitudes; and b) gradual more lasting with small amplitudes (Zhu, 2017). Only abrupt changes are considered in this study.

Characterization of the nature of change was scored using a visual assessment of the intensity/probability class of changes. The classes adopted are as follows:

– high intensity/probability: pixel for which at least one certain change is of high intensity leading or not to the conversion to a new land cover class. This is a clearly identifiable change on Landsat images corresponding, for example, to a fire or a high intensity clear-cut or partial cut of forests, to a drying of a lake, etc.;

– low to medium intensity/probability: a pixel in which the most significant certain change in terms of magnitude is of low intensity, or a pixel in which the probability of the most significant potential change is medium to low, making it difficult to detect on Landsat images due to the magnitude of the event, spatial resolution, image frequency, the presence of noise reducing image frequency, such as clouds, and SLC associated issues. Changes in this intensity/probability class do not result in conversion to other land cover classes.

– very low intensity/probability: pixel with potential changes whose probability of presence is very low and therefore very difficult to ensure their presence for the same reasons raised for the previous class. Also, changes in this intensity/probability class do not lead to conversion to other land cover classes.

Land cover for 2020 and 1984. The assignment of a single land cover class throughout the full mini time series of the year in question is used to identify land cover for each pixel. For 2020, it was based on: 1) interpretation of the year 2020 high resolution images once available, 2) exploitation and interpretation of previous GE images when changes did not lead to a conversion to other land cover types based on time series analysis, 3) exploitation of GE pictures, 4) exploitation of Landsat images acquired in 2020, at a frequency of one image taken on or around the first of each month, when the GE image(s) taken in 2020 as well as the Landsat image on or around the first of June do not allow us to identify the land cover class which was known for the past years (for example, herbaceous and annual crops).

For the year 1984, the land cover was determined using the 2020 classification, time series graphs, the intensity/probability of change class, and interpretation of Landsat images of the pixel taking into account its adjacent landscape and its evolution over time.

Seven land cover classes were identified:

– forest: predominantly wooded formations of more than 5 m in height, with a cover greater than or equal to 10% and a forestry vocation;

– shrub: formations dominated by shrubs between 2 and 5 m in height and with a cover greater than or equal to 10%;

– herbaceous/sub-shrub: herbaceous or sub-shrub formations less than 2 m in height and with a cover greater than or equal to 10%;

– cropland: cultivated lands with annual or perennial crops including fruit trees;

– water: surfaces constantly covered with water such as rivers, dams, lakes, etc.;

– developed: built-up surfaces or infrastructures.

– barren: lands that may have vegetation but have a cover that is less than 10%.

For the classification, three classes of confidence ratings were used:

a) high: the classification is certain;

b) medium: the classification is quite accurate; and

c) low: the classification is uncertain.

Due to difficulties in identifying land cover classes for both years (1984 and 2020) or one of them, or because of suspected conversions to other land cover classes in 2020, eighteen pixel-points were eliminated in the land cover study.

Tools. The processing of the Landsat images archive was substantially facilitated by the adoption of Google Earth Engine (GEE). This is a cloud computing platform accessible via a web-based application programming interface (API) and a web-based interactive development environment (Gorelick et al., 2017; Tamiminia et al., 2020). It allows access and visualization of a 40+ years archive consisting of millions of datasets including Landsat 4-8, MODIS, and Sentinel (1-3 and 5P) images among others (Amani et al., 2020). GEE also allows for automatic mass and parallel processing on Google CPUs and GPUs (Gorelick et al., 2017). Data processing is done through the various functions offered by GEE to perform different operations including simple mathematical operations and very advanced algorithms (Amani et al., 2020).

The GEE platform has been used for:

1) access to all Landsat 4-8 L1 images covering the period 1984–2022;

2) detection of noise due to the presence of clouds and their shadows and snow;

3) time series extraction for each sample point and each of the following bands: SWIR1, SWIR2, Red, NIR, Green, Blue;

4) brightness, greenness and wetness indices calculation for each image;

5) the construction of time series for each sample point and each index;

6) the creation of the bands and index time series graphs for each sample point;

7) the display for each point of the Landsat image extracts taken on or around the first of June for all even-numbered years of the study period as well as for the year 2021.

Results

Land cover. For 2020, the results show that cropland, shrub, herbaceous/sub-shrub and forest occupied 31.2%, 30.5%, 19.1%, and 16.3% respectively (Table 1). Developed, barren, and water account for 1.7%, 0.7%, and 0.5% respectively (Table 1). Regarding the confidence rating or quality of the classification, it is medium to high for 88.9% (Fig. 3a).

In 1984, shrub and cropland occupied 31.7% and 27% respectively, while herbaceous/sub-shrub and forest accounted for 20.8% and 16.5% respectively (Table 1). Barren, developed and water accounted for 2.4%, 1.2%, and 0.5% respectively. Regarding the classification quality, it is low for 63.8% of the pixels (Fig. 3b).

Table 1

Land cover conversion matrix between 1984 and 2020 for the 423 remaining sampled pixels

Land cover	Cropland	Forest	Shrub	Herbaceous/sub-shrub	Water	Developed	Barren	Land cover 1984
Cropland	112* (98.2%)	0	0	2** (1.8%)	0	0	0	114 (27%)
Forest	3** (4.3%)	65* (92.9%)	0	2** (2.9%)	0	0	0	70 (16.5%)
Shrub	1** (0.7%)	0	125* (93.3%)	8** (6%)	0	0	0	134 (31.7%)
Herbaceous / sub-shrub	14** (15.9%)	3** (3.4%)	1** (1.1%)	69* (78.4%)	0	1** (1.1%)	0	88 (20.8%)
Water	0	0	0	0	2* (100%)	0	0	2 (0.5%)
Developed	0	0	0	0	0	5* (100%)	0	5 (1.2%)
Barren	2** (20%)	1** (10%)	3** (30%)	0	0	1** (10%)	3* (30%)	10 (2.4%)
Land cover 2020	132 (31.2%)	69 (16.3%)	129 (30.5%)	81 (19.1%)	2 (0.5%)	7 (1.7%)	3 (0.7%)	–
Balance of changes	+15.8	-1.4	-3.7	-8	0	+40	-70	–

Note: * pixels with the same land cover class in 2020 and 1984; ** pixels converted from land cover classes of 1984 (first column) to other classes in 2020 (first row).

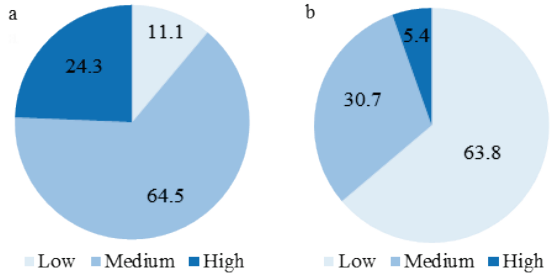

Fig. 3. Quality of the land cover classification for: *a* – the year 2020, *b* – the year 1984

Comparison of 1984 and 2020 land cover. In Table 1, the diagonal corresponds to pixels with the same land cover class in 2020 as in 1984. In this regard, land cover conversions previous to 2020 were not taken into account in this analysis. All pixels classified in the water and developed classes in 1984 remained in the same land cover class in 2020. On the other hand, 98.2%, 93.3%, 92.9%, 78.4%, and 30.0% of the pixels classified in 1984 as cropland, shrub, forest, herbaceous/sub-shrub and barren respectively had the same land cover classes in 2020.

The cells in Table 1 with double asterisks represent the loss of land cover considering the year 1984. For forest, 4.3% and 2.9% were changed to cropland and herbaceous/sub-shrub respectively. Shrub was replaced by herbaceous/sub-shrub for 6.0% and cropland for 0.7%. Herbaceous/sub-shrub was replaced essentially by cropland (15.9%) and forest (3.4%). All cropland affected by conversions was converted to herbaceous/sub-shrub for 1.8%. Shrub, cropland, forest and developed succeeded to the barren for 30%, 20%, 10% and 10% respectively.

Figure 4 illustrates the original source of the gains in 2020 regarding 1984 by land cover class. The new pixels classified as forest came from herbaceous/sub-shrub and barren for 75% and 25% respectively. Shrub gains were from 75% of barren and 25% of herbaceous/sub-shrub. Herbaceous/sub-shrub were derived from shrub, forest and cropland for 66.7%, 16.7% and 16.7% respectively. Cropland was derived from herbaceous/sub-shrub, forest, barren and shrub for 70%, 15%, 10%, 5% respectively. Newly developed pixels were derived from herbaceous/sub-shrub and barren for 50% for each class.

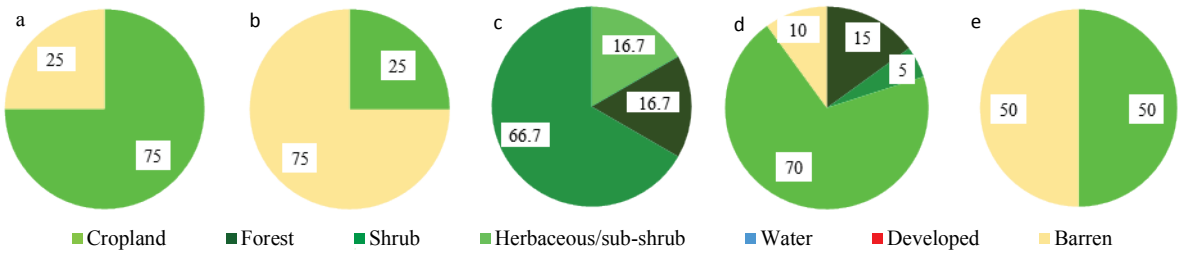

Fig. 4. Origins of gains by land cover class in 2020 compared to 1984 for: *a* – forest; *b* – shrub; *c* – herbaceous/sub-shrub; *d* – cropland; *e* – developed

The balance of changes in land cover classes regarding 1984 indicates 40.0% and 15.8% increases in developed and cropland respectively. On the other hand, decreases of 70.0%, 8.0%, 3.7% and 1.4% affected barren, herbaceous/sub-shrub, shrub and forest respectively (Table 1).

Abrupt changes. The evaluation of the abrupt changes for the 423 remaining pixel-points revealed 1921 events that affected 407 pixels (96.2%) with an average of 4.7 changes/pixel and a maximum of 10 changes. Figure 5 represents the distribution of the investigated pixels by the number of identified changes. During the study period 1984–2021, 53.9% of the pixels had 4–6 alterations, while 24.6% of the pixels had 1–3 disturbances and only 17.7% of the pixels had 7 or more changes.

In terms of the annual number of abrupt changes detected, three maxima were observed in 1990, 1999, and 2010, with a general declining tendency (Fig. 6a). With respect to the intensity and/or probability of observed changes, they were high for only 14% of the pixel points, low to medium for 49.9%, and extremely low for 36.1% (Fig. 6b). The investigation of the year of the first event (Fig. 7a) revealed that 63.9% of the pixels had their first changes between 1985 and 1990, 30.5% between 1991 and 1999 and only 5.7% between 2000 and 2014. As for the year of the last change (Fig. 7b), 74.0% and 23.6% of the pixels had their last changes during the periods 2012–2021 and 1995–2011 respectively while only 2.5% had their last changes between 1986–1994.

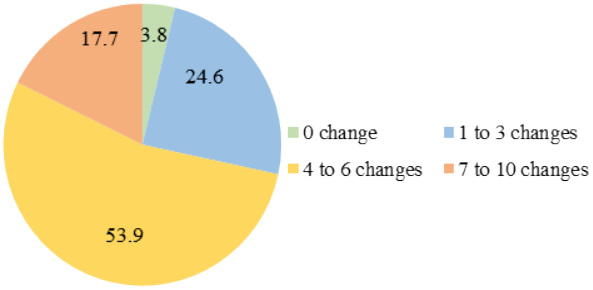

Fig. 5. Pixel distribution by class of number of observed changes from 1984 to 2021

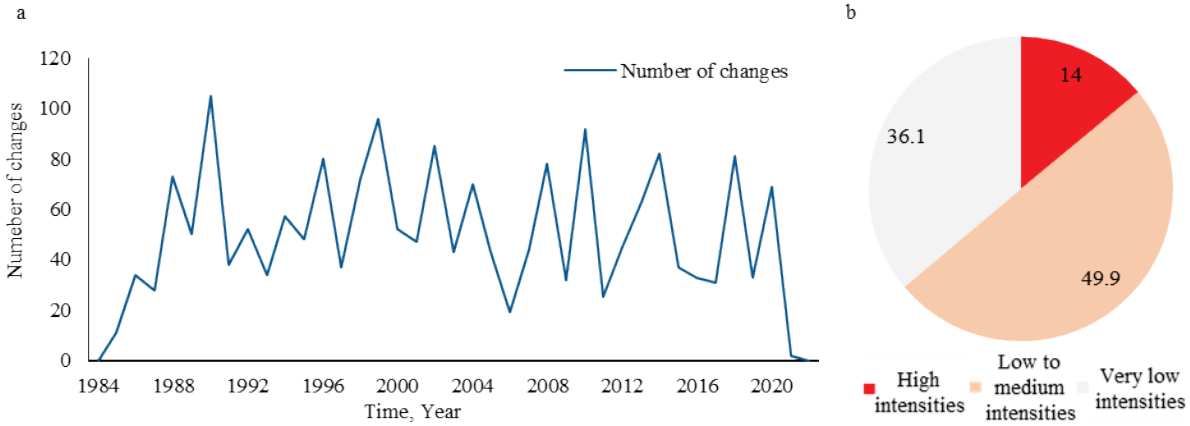

Fig. 6. Number and intensity of changes detected between 1984 and 2021:
a – evolution of the number of changes detected annually; *b* – change distribution by intensity class

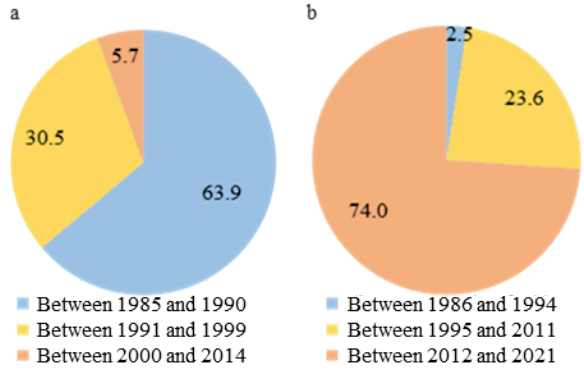

Fig. 7. Distribution of pixels per period:
a – of the first detected change; *b* – of the last detected change

Discussion

Regular long-term monitoring of the status of ecosystems is required to evaluate and better guide the different national strategies, particularly those implemented that honor Morocco's commitments in the international efforts under the UNFCCC, CBD, UNCCD and the SDGs. However, this monitoring is hampered by the lack of systematic collection of field data on these ecosystems over time and space. To address this issue, in our study, we opted for the powerful GEE cloud computing platform that offers both access to the largest archive of earth observations, which are Landsat images, large computational capabilities and a multitude of algorithms from simple to very advanced (Gorelick et al., 2017; Arevalo et al., 2020). For the examination of the image extracts on or around the first of June for the even years and 2021, the low frequency of Landsat images available in the study area required the use of images got between April and July. As a result, for the assessment of phenological differences, the extracts of successive images may not be comparable, necessitating a further search through the collection of the twenty captures. This could result in the omission of ephemeral changes that are no longer observable after two years or a false-positive detection due to the comparison of an image with an older one.

The examination of Landsat image extracts revealed the main factors causing the reduction of image quality in the study's area during the months of April to July, which are the presence of clouds and the SLC's failure. Thus, several false positive errors, related to the detection of false changes due to the presence of these noise sources, were avoided (Zhu & Woodcock, 2014a). On the other hand, the presence of these noises reduced the frequency of usable image extracts for some pixel points and even required the elimination of 59 other pixel points. The decrease in frequency affects the interpretation of the extracts and may result in change detection problems such as: a) false positive errors which occur when differences between two image extracts are exclusively due to phenological differences; b) false negative errors which happen when a relatively ephemeral change is no longer observable in the extract used; c) lateness in detecting changes.

The results for the detected abrupt changes reveal that almost all of the pixels studied, 96.2%, were affected by disturbances during the study period. However, the analysis of the intensity and probability of these changes indicates that they were high only for 14.0%, low to medium for about half of the pixels while they were very low for 36.1%. We believe that this last category of changes should be ignored because of their magnitude or because they are false positives. The study showed a general declining trend in the number of observed changes which suggests a decrease in the pressure on ecosystems. Furthermore, the availability of high-resolution GE images from the early 2000s may have contributed to the decrease in the number of uncertain changes identified on Landsat images. Regarding the year of first change, only 5.7% of the pixels had their first events after the year 2000, indicating that these pixels did not have any

changes during at least the first 16 years of the study period. However, changes affected two thirds of the pixels very early during the first six years. On the other hand, 2.5% of the pixels had their last events within the first ten years and so had no changes for at least 27 years. The years of the first late change and of the last early change provide information particularly on the absence of pressure during relatively long periods on the ecosystems, which could reflect the different orientations adopted by Morocco, particularly by the forestry administration, and which reflect the implementation of strategic plans such as the National Forestry Plan, the Protected Areas Director Plan, the National Watershed Management Plan. These strategic plans have been implemented at the local scale by the execution of conservation measures for the eradication of various forms of pressure such as income-generating activities and the compensation mechanism.

The confidence level of the land cover classification for the year 2020, is medium to high for 88.9% of the pixels, which could be judged globally satisfactory to very satisfactory. This level of satisfaction was achieved mainly due to the possibility of visual interpretation of Google Earth high resolution (HR) images. On the other hand, the land cover classification for the year 1984 was unsatisfactory for 64% of the pixels. This is due to 1) the absence of HR images for this year and the visual interpretation based on low resolution Landsat images, 2) the absence of an initial mapping or field reality of the reference period to establish a supervised classification based on the spectral characteristics of each land cover type. This could have the effect of underestimating the cases of conversions.

The assessment of land cover dynamic shows that despite the pressure on terrestrial ecosystems, about 93%, 92% and 78% of the pixels classified in 1984 as shrub, forest and herbaceous/sub-shrub had the same land cover classes in 2020. These values show that changes do not necessarily lead to conversion to other land cover classes, and also reflect the conservation efforts in terms of creation of protected areas, implementation of management plans for these areas and management of forest ecosystems and watersheds in the study area.

Analysis of forest and herbaceous/sub-shrub losses suggest that cropland is the driving force for these ecosystem conversions and even for conversions of shrub, converted primarily to herbaceous/shrubs. This latest land cover may be a transition to other land cover classes dominated by cropland. Figure 8 illustrates the conversion of a forest to cropland following partial cuttings between 2004 and 2013 as highlighted using the SWIR1 band reflectance time series, Landsat and Google Earth image extracts.

The gains of forest (exclusively from conversion of herbaceous/sub-shrub and barren), shrub (exclusively from conversion of barren and herbaceous/sub-shrub) and herbaceous/sub-shrub (partly from conversion of cropland) reflect on the one hand the capacity of ecosystems to regenerate themselves but also the efforts deployed in the rehabilitation of these ecosystems and the supporting actions that guarantee their success. Figure 9 shows an example of the rehabilitation of forest ecosystems through a plantation of a resinous species in the late 1980s (Fig. 9a). The plantation is observable on the Landsat images since 1990 (Fig. 9c). In the time series plot of the Wetness index, we note a linear increase from 1988 until the saturation of the index in 1999 corresponding to the maximum cover (Fig. 9a).

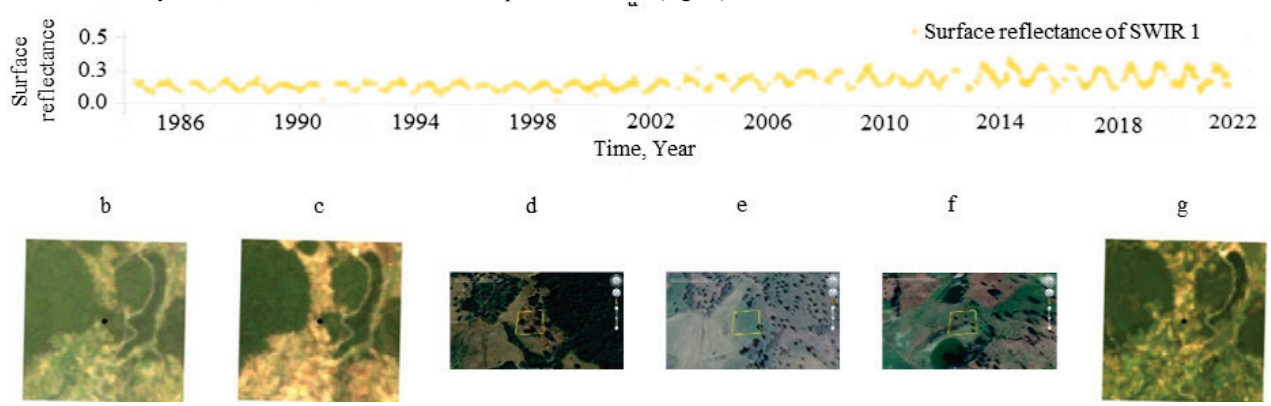

Fig. 8. Conversion of a forest into cropland for the Point-pixel n°258 (black dot in Landsat images and yellow rectangle in Google Earth images): *a* – SWIR1 Time Series graph for the period 1984–2022; natural color composite Landsat images acquired on: *b* – 05/16/2002; *c* – 07/08/2004; *g* – 05/01/2020; Google Earth images captured in: *d* – 08/2007; *e* – 03/2014; *f* – 02/2020

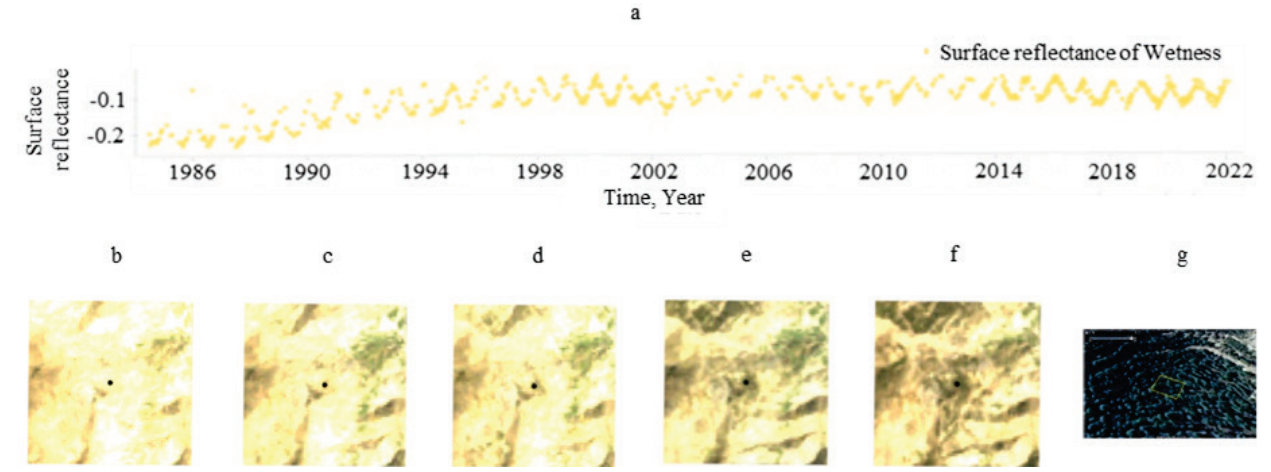

Fig. 9. Evolution of a plantation that occurred in late 1980s for the Point-pixel n°99 (Black dot in Landsat images and yellow rectangle in Google Earth image): *a* – Wetness Time Series graph for the period 1984–2022; natural color composite Landsat images acquired on: *b* – 06/08/1984; *c* – 04/22/1990; *d* – 05/24/1996; *e* – 04/12/2004; *f* – 05/02/2020; *g* – Google Earth image captured in 12/2020

The balance of conversions (losses and gains), shows that there was a very strong decrease in barren essentially in favour of forest and cropland, with only a minor decrease in herbaceous/sub-shrub, shrub and forest. On the other hand, developed (whose new land comes exclusively from barren and herbaceous/sub-shrub) and cropland (whose new land comes mainly from herbaceous/sub-shrub and secondarily from forest and shrub) have experienced high and weak increases respectively. Furthermore, Chebli et al. (2018) in their study of the provinces of Chefchaouen, Tetou-

an, M'diq-Fnideq, Fahs-Anjra, Tangier, Larach and Ouazzane, revealed a regressive dynamic of forest ecosystems compensated by a conversion of matorral to forest and agricultural land. In consideration of the incomparability of numbers, methodologies and temporalities, and given that for our study the detection of conversions depends on the identification of changes through the interpretation of time series of all available images covering the period 1984–2020 by exploiting the extracts of Landsat images as well as the pattern of time series derived from reflectances, to assess the intensity of changes and their characterization, the overall trends are very similar.

Although the findings of the study are important for understanding the dynamic and guiding the decision makers, future perspectives could be proposed to overcome the difficulties encountered particularly by automating the change detection and classification process which should allow among other things:

– taking phenology into account (Brooks et al., 2013);

– exploiting an optimal number of images or even all available Landsat images and allowing one to deal with the computational and storage constraints of the images (Brooks et al., 2013; Kennedy et al., 2018);

– adopting a robust approach for land cover classification and identifying potential conversions (Zhu et al., 2016).

Conclusion

The present paper revealed that almost the entire study area was affected by changes over the study period with around one third of them which can be ignored due to their magnitudes or because they are false positives. The study revealed a general downward trend in the changes detected, which particularly reflects a decrease in the pressure on the different ecosystems. The assessment of land cover dynamic showed that despite the pressure on terrestrial ecosystems, the majority of the pixels classified in 1984 as shrub, forest and herbaceous/sub-shrub did not undergo conversion. These results are particularly indicative of Morocco's conservation efforts. The study indicates that cropland is the main driving force for conversion of forest, herbaceous/sub-shrub and even shrub. The gains for the latter three ecosystems reflect both the power of these ecosystems to regenerate themselves and the kingdom's rehabilitation efforts. Thus, the balance of losses and gains for these ecosystems shows a slight decrease in their respective areas.

References

Amani, M., Ghorbanian, A., Ahmadi, S. A., Kakooei, M., Moghimi, A., Mirmazloumi, S. M., Moghaddam, S. H. A., Mahdavi, S., Ghahremanloo, M., Parsian, S., Wu, Q., & Brisco, B. (2020). Google earth engine cloud computing platform for remote sensing big data applications: A comprehensive review. Institute of Electrical and Electronics Engineers Journal of Selected Topics in Applied Earth Observations and Remote Sensing, 13, 5326–5350.

Arevalo, P., Bullock, E., Woodcock, C., & Olofsson, P. (2020). A suite of tools for continuous land change monitoring in google earth engine. Frontiers in Climate, 2, 1–19.

Azedou, A., Amine, A., Kisekka, I., Lahssini, S., Bouziani, Y., & Moukrim, S. (2023). Enhancing land cover/land use (LCLU) classification through a comparative analysis of hyperparameters optimization approaches for deep neural network (DNN). Ecological Informatics, 78, 102333.

Banskota, A., Kayastha, N., Falkowski, M. J., Wulder, M. A., Froese, R. E., & White, J. C. (2014). Forest monitoring using Landsat time series data: A review. Canadian Journal of Remote Sensing, 40(5), 362–384.

Benabid, A. (2000). Flore et écosystèmes du Maroc: Évaluation et préservation de la biodiversité [Flora and ecosystems of Morocco: Evaluation and preservation of biodiversity]. Ibis Press, Paris (in French).

Benabou, A., Moukrim, S., Lahssini, S., Aboudi, A. E., Menzou, K., Elmalki, M., Madihi, M. E., & Rhazi, L. (2022). Impact of climate change on potential distribution of *Quercus suber* in the conditions of North Africa. Biosystems Diversity, 30(3), 289–294.

Brooks, E. B., Wynne, R. H., Thomas, V. A., Blinn, C. E., & Coulston, J. W. (2014). On-the-fly massively multitemporal change detection using statistical quality control charts and Landsat data. IEEE Transactions on Geoscience and Remote Sensing, 52(6), 3316–3332.

Brown, J. F., Tollerud, H. J., Barber, C. P., Zhou, Q., Dwyer, J. L., Vogelmann, J. E., Loveland, T. R., Woodcock, C. E., Stehman, S. V., Zhu, Z., Pengra, B. W., Smith, K., Horton, J. A., Xian, G., Auch, R. F., Sohl, T. L., Sayler, K. L., Gallant, A. L., Zelenak, Reker, R. R., & Rover, J. (2020). Lessons learned implementing an operational continuous United States national land change monitoring capability: The land change monitoring, assessment, and projection (LCMAP) approach. Remote Sensing of Environment, 238, 111356.

Carpenter, S. R., DeFries, R., Dietz, T., Mooney, H. A., Polasky, S., Reid, W. V., & Scholes, R. J. (2006). Millennium ecosystem assessment: Research needs. Science, 314(5797), 257–258.

Chance, C. M., Hermosilla, T., Coops, N. C., Wulder, M. A., & White, J. C. (2016). Effect of topographic correction on forest change detection using spectral trend analysis of Landsat pixel-based composites. International Journal of Applied Earth Observation and Geoinformation, 44, 186–194.

Chebli, Y., Chentouf, M., Ozer, P., Hornick, J.-L., & Cabaraux, J.-F. (2018). Forest and silvopastoral cover changes and its drivers in Northern Morocco. Applied Geography, 101, 23–35.

Coppin, P., Jonckheere, I., Nackaerts, K., Muys, B., & Lambin, E. (2004). Digital change detection methods in ecosystem monitoring: A review. International Journal of Remote Sensing, 25(9), 1565–1596.

Crist, E. P. (1985). A TM Tasseled Cap equivalent transformation for reflectance factor data. Remote Sensing of Environment, 17(3), 301–306.

Díaz, S. M., Settele, J., Brondízio, E., Ngo, H., Guèze, M., Agard, J., Arneth, A., Balvanera, P., Brauman, K., & Butchart, S. (2019). The global assessment report on biodiversity and ecosystem services. Intergovernmental Science-Policy Platform on Biodiversity and Ecosystem Services. United Nations Environment Programme, Nairobi.

Frazier, R. J., Coops, N. C., & Wulder, M. A. (2015). Boreal shield forest disturbance and recovery trends using Landsat time series. Remote Sensing of Environment, 170, 317–327.

Fu, P., & Weng, Q. (2016). A time series analysis of urbanization induced land use and land cover change and its impact on land surface temperature with Landsat imagery. Remote Sensing of Environment, 175, 205–214.

Gao, B.-C. (1996). NDWI – a normalized difference water index for remote sensing of vegetation liquid water from space. Remote Sensing of Environment, 58(3), 257–266.

Gorelick, N., Hancher, M., Dixon, M., Ilyushchenko, S., Thau, D., & Moore, R. (2017). Google earth engine: Planetary-scale geospatial analysis for everyone. Remote Sensing of Environment, 202, 18–27.

Gutman, G., Janetos, A. C., Justice, C. O., Moran, E. F., Mustard, J. F., Rindfuss, R. R., Skole, D., Turner II, B. L., & Cochrane, M. A. (2004). Land change science: Observing, monitoring and understanding trajectories of change on the earth's surface. Springer Science & Business Media. Vol. 6.

Halabisky, M., Moskal, L. M., Gillespie, A., & Hannam, M. (2016). Reconstructing semi-arid wetland surface water dynamics through spectral mixture analysis of a time series of Landsat satellite images (1984–2011). Remote Sensing of Environment, 177, 171–183.

Hamunyela, E., Verbesselt, J., & Herold, M. (2016). Using spatial context to improve early detection of deforestation from Landsat time series. Remote Sensing of Environment, 172, 126–138.

Hansen, M. C., Potapov, P. V., Moore, R., Hancher, M., Turubanova, S. A., Tyukavina, A., Thau, D., Stehman, S. V., Goetz, S. J., Loveland, T. R., Kommareddy, A., Egorov, A., Chini, L., Justice, C. O., & Townshend, J. R. G. (2013). High-resolution global maps of 21st-century forest cover change. Science, 342(6160), 850–853.

Houghton, R. A., & Nassikas, A. A. (2017). Global and regional fluxes of carbon from land use and land cover change 1850–2015. Global Biogeochemical Cycles, 31(3), 456–472.

Jin, S., & Sader, S. A. (2005). MODIS time-series imagery for forest disturbance detection and quantification of patch size effects. Remote Sensing of Environment, 99(4), 462–470.

Kennedy, R. E., Yang, Z., Cohen, W. B., Pfaff, E., Braaten, J., & Nelson, P. (2012). Spatial and temporal patterns of forest disturbance and regrowth within the area of the Northwest Forest Plan. Remote Sensing of Environment, 122, 117–133.

Kennedy, R. E., Yang, Z., Gorelick, N., Braaten, J., Cavalcante, L., Cohen, W. B., & Healey, S. (2018). Implementation of the LandTrendr algorithm on Google earth engine. Remote Sensing, 10(5), 691.

Kibret, K. S., Marohn, C., & Cadisch, G. (2016). Assessment of land use and land cover change in South Central Ethiopia during four decades based on integrated analysis of multi-temporal images and geospatial vector data. Remote Sensing Applications: Society and Environment, 3, 1–19.

Masek, J. G., Vermote, E. F., Saleous, N. E., Wolfe, R., Hall, F. G., Huemmrich, K. F., Gao, F., Kutler, J., & Lim, T. K. (2006). A Landsat surface reflectance dataset for North America, 1990–2000. IEEE Geoscience and Remote Sensing Letters, 3(1), 68–72.

Moukrim, S., Lahssini, S., Naggar, M., Lahlaoi, H., Rifai, N., Arahou, M., Rhazi, L., Moukrim, S., Lahssini, S., Naggar, M., Lahlaoi, H., Rifai, N., Arahou, M., & Rhazi, L. (2019). Local community involvement in forest rangeland management: Case study of compensation on forest area closed to grazing in Morocco. The Rangeland Journal, 41(1), 43–53.

Moukrim, S., Lahssini, S., Rhazi, M., Menzou, K., El Madihi, M., Rifai, N., Bouziani, Y., Azedou, A., Boukhris, I., & Rhazi, L. (2022). Climate change impact on potential distribution of an endemic species Trabut. Ekológia (Bratislava), 41(4), 329–339.

Pereira, H. M., Ferrier, S., Walters, M., Geller, G. N., Jongman, R. H. G., Scholes, R. J., Bruford, M. W., Brummitt, N., Butchart, S. H. M., Cardoso, A. C., Coops, N. C., Dulloo, E., Faith, D. P., Freyhof, J., Gregory, R. D., Heip, C., Höft, R., Hurtt, G., Jetz, W., Karp, D. S., McGeoch, M. A., Obura, D., Onoda, Y., Pettorelli, N., Reyers, B., Sayre, R., Scharlemann, J. P. W., Stuart, S. N., Turak, E., Walpole, M., & Wegmann, M. (2013). Essential biodiversity variables. Science, 339(6117), 277–278.

Reed, B. C., Brown, J. F., VanderZee, D., Loveland, T. R., Merchant, J. W., & Ohlen, D. O. (1994). Measuring phenological variability from satellite imagery. Journal of Vegetation Science, 5(5), 703–714.

Scholes, R. J., Walters, M., Turak, E., Saarenmaa, H., Heip, C. H., Tuama, É. Ó., Faith, D. P., Mooney, H. A., Ferrier, S., Jongman, R. H., Harrison, I. J., Yahara, T., Pereira, H. M., Larigauderie, A., & Geller, G. (2012). Building a global observing system for biodiversity. Current Opinion in Environmental Sustainability, 4(1), 139–146.

Secades, C., O'Connor, B., Brown, C., & Walpole, M. (2014). Earth observation for biodiversity monitoring: A review of current approaches and future opportunities for tracking progress towards the Aichi Biodiversity Targets. CBD Technical Series, 72. Secretariat of the Convention on Biological Diversity, Montreal.

Singh, A. (1989). Review article digital change detection techniques using remotely-sensed data. International Journal of Remote Sensing, 10(6), 989–1003.

Skidmore, A. K., Coops, N. C., Neinavaz, E., Ali, A., Schaepman, M. E., Paganini, M., Kissling, W. D., Vihervaara, P., Darvishzadeh, R., Feilhauer, H., Fernandez, M., Fernández, N., Gorelick, N., Geijzendorffer, I., Heiden, U., Heurich, M., Hobern, D., Holzwarth, S., Muller-Karger, F. E., Kerchove, R. V. D., Lausch, A., Leitão, P. J., Lock, M. C., Mücher, C. A., O'Connor, B., Rocchini, D., Roeoesli, C., Turner, W., Vis, J. K., Wang, T., Wegmann, M., & Wingate, V. (2021). Priority list of biodiversity metrics to observe from space. Nature Ecology and Evolution, 5(7), 896–906.

Tamiminia, H., Salehi, B., Mahdianpari, M., Quackenbush, L., Adeli, S., & Brisco, B. (2020). Google earth engine for geo-big data applications: A meta-analysis and systematic review. International Society for Photogrammetry and Remote Sensing Journal of Photogrammetry and Remote Sensing, 164, 152–170.

Turner, B. L., Lambin, E. F., & Reenberg, A. (2007). The emergence of land change science for global environmental change and sustainability. Proceedings of the National Academy of Sciences, 104(52), 20666–20671.

Verbesselt, J., Hyndman, R., Zeileis, A., & Culvenor, D. (2010). Phenological change detection while accounting for abrupt and gradual trends in satellite image time series. Remote Sensing of Environment, 114(12), 2970–2980.

Vermote, E., Justice, C., Claverie, M., & Franch, B. (2016). Preliminary analysis of the performance of the Landsat 8/OLI land surface reflectance product. Remote Sensing of Environment, 185, 46–56.

Wulder, M. A., Masek, J. G., Cohen, W. B., Loveland, T. R., & Woodcock, C. E. (2012). Opening the archive: How free data has enabled the science and monitoring promise of Landsat. Remote Sensing of Environment, 122, 2–10.

Wulder, M. A., White, J. C., Goward, S. N., Masek, J. G., Irons, J. R., Herold, M., Cohen, W. B., Loveland, T. R., & Woodcock, C. E. (2008). Landsat continuity: Issues and opportunities for land cover monitoring. Remote Sensing of Environment, 112(3), 955–969.

Zhu, Z. (2017). Change detection using landsat time series: A review of frequencies, preprocessing, algorithms, and applications. International Society for Photogrammetry and Remote Sensing Journal of Photogrammetry and Remote Sensing, 130, 370–384.

Zhu, Z., & Woodcock, C. E. (2014a). Automated cloud, cloud shadow, and snow detection in multitemporal Landsat data: An algorithm designed specifically for monitoring land cover change. Remote Sensing of Environment, 152, 217–234.

Zhu, Z., & Woodcock, C. E. (2014b). Continuous change detection and classification of land cover using all available Landsat data. Remote Sensing of Environment, 144, 152–171.

Zhu, Z., Gallant, A. L., Woodcock, C. E., Pengra, B., Olofsson, P., Loveland, T. R., Jin, S., Dahal, D., Yang, L., & Auch, R. F. (2016). Optimizing selection of training and auxiliary data for operational land cover classification for the LCMAP initiative. International Society for Photogrammetry and Remote Sensing Journal of Photogrammetry and Remote Sensing, 122, 206–221.

Zhu, Z., Woodcock, C. E., Holden, C., & Yang, Z. (2015). Generating synthetic Landsat images based on all available Landsat data: Predicting Landsat surface reflectance at any given time. Remote Sensing of Environment, 162, 67–83.

Zhu, Z., Zhang, J., Yang, Z., Aljaddani, A. H., Cohen, W. B., Qiu, S., & Zhou, C. (2020). Continuous monitoring of land disturbance based on Landsat time series. Remote Sensing of Environment, 238, 111–116.